Available online at www.sciencedirect.com
SciVerse ScienceDirect
www.elsevier.com/locate/brainres

Research Report

Altered auditory processing in a mouse model of fragile X syndrome

*Sarah Rotschafer, Khaleel Razak**

Graduate Neuroscience Program and Department of Psychology, University of California, Riverside, CA, USA

ARTICLE INFO

Article history:
Accepted 18 February 2013
Available online 28 February 2013

Keywords:
Auditory cortex
Fragile X syndrome
Autism
Fmr1 KO mice
Hyper-excitability

ABSTRACT

This study provides the first description of auditory cortical processing in a mouse model of Fragile X Syndrome (FXS). FXS is a genetic cause of intellectual impairment and is an autism spectrum disorder. Human studies with auditory evoked potentials indicate that FXS is associated with abnormal auditory processing. The *Fmr1* knock-out (KO) mouse is a useful model for studying FXS. The KO mice show acoustic hypersensitivity and propensity for audiogenic seizures, suggesting altered auditory responses. However, the nature of changes at the neuronal level is not known. Here we conducted *in vivo* single unit extracellular electrophysiology in the auditory cortex of urethane/xylazine-anesthetized *Fmr1* KO mice in response to tones and frequency modulated (FM) sweeps. Using tones as stimuli, we report expanded frequency tuning, enhanced response magnitude, and more variable first spike latencies in *Fmr1* KO mice compared to wild-type controls. FM sweep stimuli revealed altered sensitivity to the rate of frequency change indicating abnormal spectrotemporal processing. There was no difference in FM sweep direction selectivity. Consistent with studies of the somatosensory cortex, these data point to hyper-responsiveness of auditory neurons as a key processing abnormality in FXS. Auditory neural responses can serve as outcome measures in preclinical trials of therapeutics for FXS as well as serve as physiological probes to study their mechanisms of action.

1. Introduction

Fragile X Syndrome (FXS) is a genetic disorder that affects 1 in every 4000 males and 1 in every 8000 females (Hagerman, 2008). FXS results from elongated CGG trinucleotide repeats in the promoter region of the *FMR1* gene which become hypermethylated, leading to inactivation of the *FMR1* gene and a failure to produce fragile X mental retardation protein (FMRP) (O'Donnell and Warren, 2002). FMRP acts to inhibit the translation of several synaptic mRNAs, and loss of FMRP typically results in an over-production of associated synaptic proteins (Bassell and Warren, 2008). The symptoms of FXS include altered social interactions, hyperactivity, hypersensitivity to sensory stimuli, repetitive behavior, abnormal dendritic spine formation, intellectual disability, language deficits and seizures (Largo and Schinzel, 1985; Hanson et al., 1986; Roberts et al., 2001, 2007;

Abbreviations: A1, primary auditory cortex; AAF, anterior auditory field; AP, all pass; BP, band pass; CF, characteristic frequency; DSI, direction selectivity index; FM, frequency modulated; FMRP, fragile X mental retardation protein; FP, fast pass; FXS, fragile X syndrome; KO, knock out; MT, minimum threshold; RTI, rate tuning index; SP, slow pass; WT, wild type

**Corresponding author.* Fax: +1 951 827 3985.
E-mail address: khaleel@ucr.edu (K. Razak).

0006-8993/$ - see front matter © 2013 Elsevier B.V. All rights reserved.
http://dx.doi.org/10.1016/j.brainres.2013.02.038

Fidler et al., 2007; Barnes et al., 2009). FXS is a known genetic cause of autism spectrum disorders (Hagerman, 2008).

FXS patients also display an array of auditory cortex structural and functional abnormalities. There is a reduction in size of the superior temporal gyrus in FXS (Reiss et al., 1994) and a temporal lobe-specific white matter enlargement (Hazlett et al., 2012). Brain activity of FXS patients is diffuse due to activation of more areas in the brain than typically seen in controls when presented with tones (Hall et al., 2011). Electroencephalogram (EEG) studies have demonstrated that FXS patients have enlarged N1 and N2 components when presented with deviant tone stimuli (Castren et al., 2003; Van der Molen et al.,2012a, 2012b), and show unusually slow background rhythm (Wisniewski et al., 1991). N1 is typically associated with activity within the superior temporal gyrus (Scherg and von Cramon, 1986; O'Connor, 2012). Using magnetoencephalography (MEG), Rojas and colleagues showed that the N100 component was enhanced during an auditory oddball task (Rojas et al., 2001). The nature of neuronal deficits in the auditory system that may lead to altered EEG and MEG signals remains unclear.

The goal of the present study was to determine auditory response selectivity at the level of individual neurons in the primary auditory cortex (A1) and the anterior auditory field (AAF) of the *Fmr1* knock-out (KO) mouse and compare responses with wild-type (WT) controls. *Fmr1* KO mice display several symptoms associated with FXS, and is the commonly used mouse model for FXS. As in humans with FXS, *Fmr1* KO mice display abnormal dendritic spine maturation in cortex and hippocampus (Galvez et al., 2003; McKinney et al., 2005; Grossman et al., 2006, 2010; Cruz-Martin et al., 2010; Pan et al., 2010). There is also evidence that *Fmr1* KO mice show social deficits when interacting with other mice, and engage in repetitive behaviors (Mineur et al., 2002; Spencer et al., 2005; Crawley, 2007) and show abnormal social vocalizations (Rotschafer et al., 2012). In the auditory brainstem, FMRP contributes to maintenance of tonotopic gradients in potassium ion channels and KO mice show deficits in experience-dependent plasticity (Strumbos et al., 2010). *Fmr1* KO mice also show audiogenic seizures and hypersensitivity to auditory stimuli (Musumeci et al., 2000; Chen and Toth, 2001; Errijgers et al., 2008) as seen in human

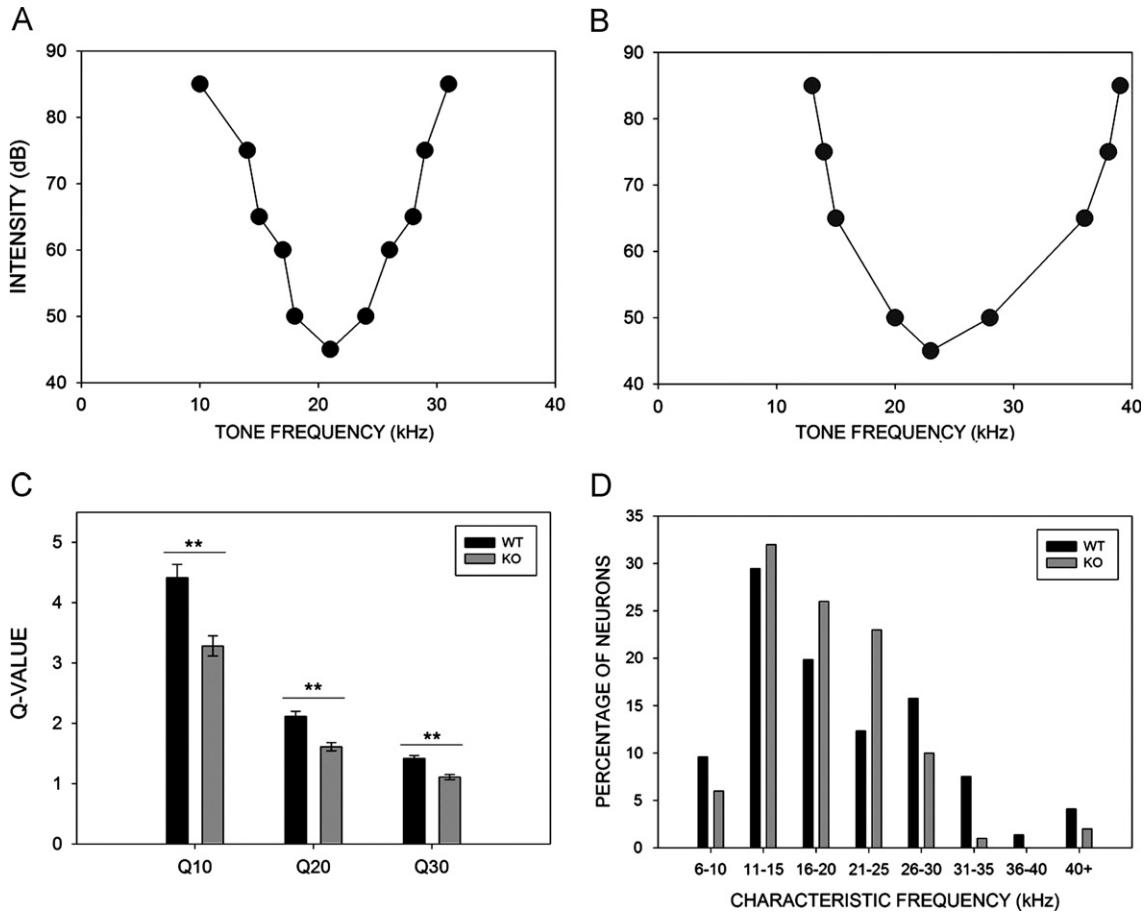

Fig. 1 – Neurons from *Fmr1* KO mice show significantly broader frequency tuning and lower Q-values than WT mice. Examples of frequency tuning curves from a WT neuron (A) and a KO neuron (B). The example neurons are of comparable CF and threshold, however, the KO neuron is more broadly tuned. (C). Q-values at 10, 20, and 30 dB above threshold were significantly smaller in KO mice neurons compared to WT mice neurons (WT: $n=127$ neurons, KO: $n=97$ neurons). This indicates broader frequency tuning in KO mouse cortex. (D) WT and KO neurons sampled did not show significant differences in the distribution of characteristic frequency ($P<0.01$).**

FXS patients (Hagerman et al., 1986, 1991; Miller et al., 1999; Frankland et al., 2004; Hessl et al., 2009; Yuhas et al., 2011). This suggests abnormal responses in the auditory system of the *Fmr1* KO mice, but the neural correlates of such deficits have not been previously investigated.

In vitro studies of the *Fmr1* KO mice somatosensory cortex have shown abnormalities in the balance between inhibition and excitation in cortical circuits (Gibson et al., 2008, Hays et al., 2011, Paluszkiewicz et al., 2011). Such an imbalance has been postulated as a general mechanism underlying symptoms in several neurodevelopmental disorders (Rubenstein and Merzenich, 2003). It is not known if the auditory cortex in *Fmr1* KO mice shows similar changes, but the auditory processing deficits seen in both FXS patients and the *Fmr1* KO mice formed the motivation to examine *in vivo* response selectivity in the auditory cortex. We compared four response properties from single unit recordings across the WT and KO mice: frequency tuning, response magnitude to tones, variability in response latencies and response selectivity for frequency modulated (FM) sweep direction and rate. These properties allow an evaluation of spectral, temporal and spectrotemporal processing in the cortex. We found that *Fmr1* KO mouse neurons had significantly broader frequency tuning curves, more jitter in the first spike latency, stronger excitatory response to tones and altered selectivity for FM sweep. However, there was no difference in FM sweep direction selectivity. The changes in auditory response selectivity may explain observed changes in auditory processing in FXS patients and altered sound-driven behaviors in the *Fmr1* KO mice.

Table 1 – Distribution of cortical depths from which recordings were obtained.

Depth (μm)	WT (%)	KO (%)
200–299	19.49	12.05
300–499	38.98	46.99
500–700	41.53	40.96

2. Results

The main goal of this study was to compare responses of neurons in primary auditory cortex (A1) and anterior auditory field (AAF) to tones and FM sweeps between the *Fmr1* knockout (KO) mice and wild-type controls (WT).

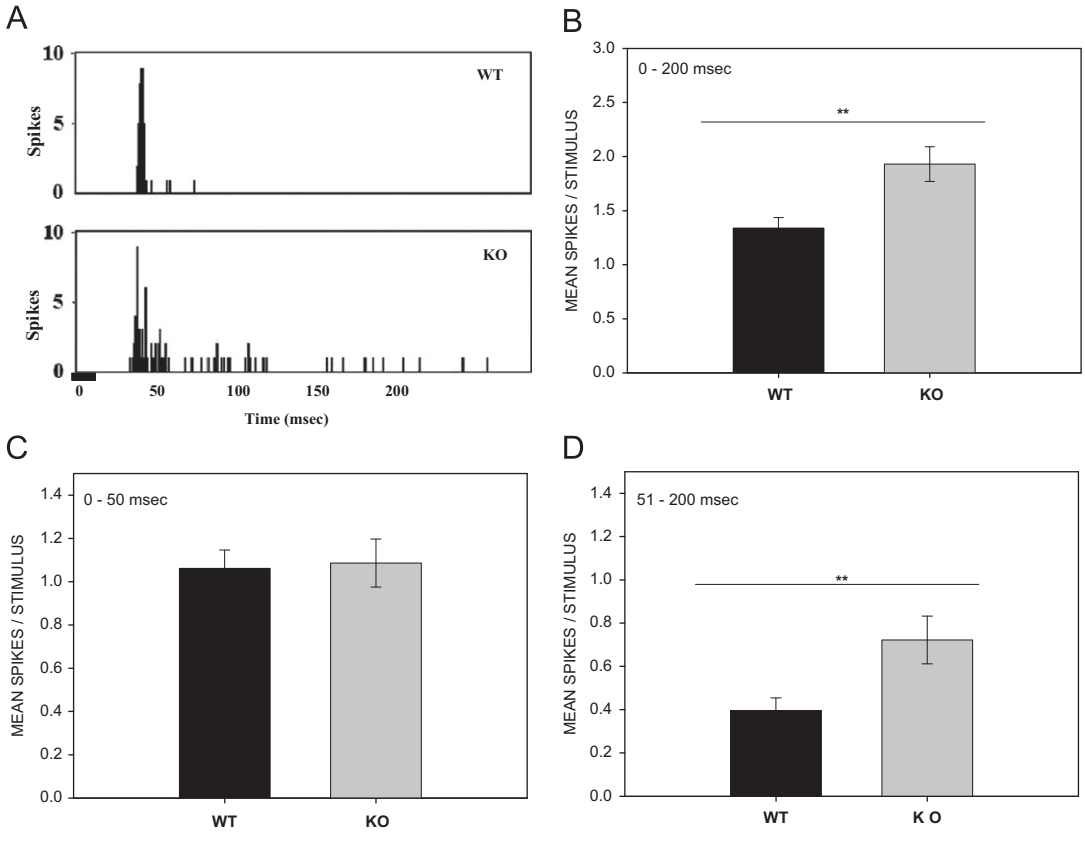

Fig. 2 – *Fmr1* KO neurons show a significantly larger response magnitude than WT neurons in response to the CF tone. (A) Post-stimulus time histogram (PSTH) in response to a 10 ms CF tone in example WT and KO neurons. The stimulus onset and duration are indicated by the black bar under the PSTHs. The CF tone elicits a robust response in both wild type and *Fmr1* KO neurons, with KO neurons displaying a more prolonged response. (B) KO neurons ($n=51$) show a greater response magnitude than WT neurons ($n=67$) when the entire 200 ms recording window was compared. (C) There was no significant difference between groups in the first 50 ms following stimulus onset. (E) The enhanced response seen in KO neurons was the result of increased activity in the 51–200 ms window following stimulus onset.

2.1. *Fmr1 KO neurons are more broadly tuned than WT neurons*

Q-values for 205 neurons from WT mice and 134 neurons from KO mice at 10, 20, and 30 dB above threshold were compared. Example tuning curves typical of WT and KO mouse cortex are shown in Fig. 1A and B. Across the population, frequency tuning in KO mice was broader than in WT mice (Fig. 1C, one-way ANOVA $F(5782)=86.063$, $p<0.001$). Neither the distribution of CF ($\chi^2=28$, $p=0.260$, Fig. 1D) nor the cortical depths of recording ($\chi^2=6$, $p=0.199$, Table 1) were significantly different between WT and KO mice, indicating that the broader tuning in the KO neurons was not an artifact of differences in recording depth or tonotopic location bias. The minimum threshold (MT) for tone responses were also not significantly different between the two groups (t-test, $p=0.231$) indicating that threshold sensitivity is not affected in KO mice.

2.2. *Fmr1 KO neurons produce more spikes and show a larger variability in first spike latency*

Fmr1 KO mice are acoustically hypersensitive and are prone to audiogenic seizures (Chen and Toth, 2001; Nielsen et al., 2002; Frankland et al., 2004), suggesting enhanced excitability in the auditory system. To test this, the magnitude of response to the characteristic frequency (CF) tone was compared. Fig. 2A provides an example of WT and KO neuronal response to 10 ms single frequency tone stimulus presented at characteristic frequency. When response magnitude was compared across the entire 200 ms recording window, neurons from KO mice showed a significant enhancement in response magnitude (Fig. 2B, Mann–Whitney Rank Sum Test, $p=0.002$). This enhancement was carried by changes in response magnitude during the latter portion (51–200 ms, Fig. 2D, Mann–Whitney Rank Sum Test, $p=0.002$) of response and not due to changes in the first 50 ms of responses (Fig. 2C, Mann–Whitney Rank Sum Test, $p=0.916$). The mean first spike latency was not significantly different in KO mice (Fig. 3A, Mann–Whitney Rank Sum Test, $p=0.09$), and was less than 50 ms in the majority of neurons. These data suggest an inability of KO neurons to shut down activity following an initial onset-related burst. First spike latency was also more variable in KO mouse neurons. Fano factor was larger in KO neurons (Mann–Whitney Rank Sum Test, $p=0.027$, Fig. 3B) suggesting reduced temporal precision of excitatory tone representation in KO neurons.

2.3. *Frequency modulated sweep rate selectivity*

Frequency modulated (FM) sweep rate selectivity was tested in 155 WT neurons and 101 KO neurons, using upward and downward FM sweeps with sweep rates between 0.2 to 45 kHz/ms. Neuronal response was classified as being fast pass (FP, Fig. 4A), band pass (BP, Fig. 4B), all pass (AP, Fig. 4C), or slow pass (SP Fig. 4D). No significant difference was found for the distribution of FM rate selectivity types to upward ($\chi^2=13.543$, $p=0.140$) or downward ($\chi^2=5.890$, $p=0.751$) FM sweeps across WT and KO mice (Fig. 4E and F).

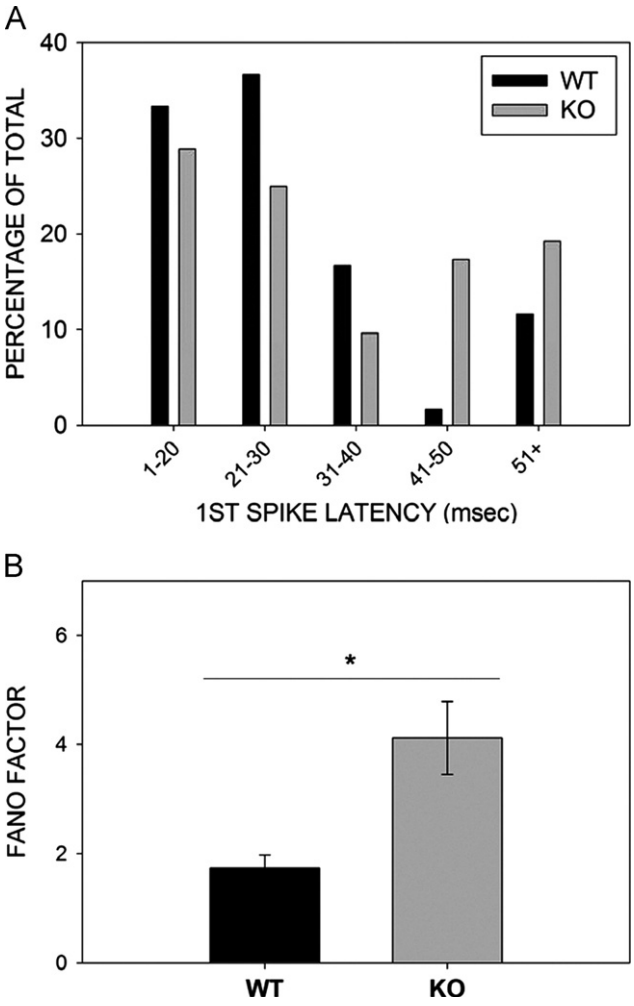

Fig. 3 – Distribution of first spike latency and variability of first spike latency in response to CF tone in WT and KO mouse neurons. (A) In both groups, the first spike occurred within the first 50 ms of stimulus onset in the majority of neurons. (B) *Fmr1* KO neurons show greater variability in first spike latency. KO neurons ($n=51$) demonstrate a larger Fano factor than WT neurons ($n=67$).

Cortical neurons in KO mice were, however, less selective for FM sweep rates compared to WT neurons. The rate tuning index (RTI) was used as a measure of FM rate selectivity (Godey et al., 2005; Trujillo et al., 2011). Both BP (one-way ANOVA $F(3,80)=6.988$, $p<0.001$) and FP (one-way ANOVA $F(3,133)=21.584$, $p<0.001$) neurons in KO mice demonstrated smaller mean RTI values in response to upward and downward FM sweeps than WT neurons (Fig. 5A and B, respectively). No significant differences were seen in the RTI values of SP (Fig. 4C, one-way ANOVA $F(3,72)=0.795$, $p=0.501$) or AP neurons (Fig. 5D, one-way ANOVA $F(3,138)=0.416$, $p=0.742$).

The reduced rate selectivity may arise due to the fact that neurons respond better to slower and/or faster sweeps in KO mice than WT mice. To distinguish between these possibilities, the 50% cut-off rate was measured (*e.g.*, Fig. 6A). This measure provides information on the fastest and the slowest sweep rates that produce more than 50% of maximum response. For fast-pass neurons only the 'slow' 50% cut-off

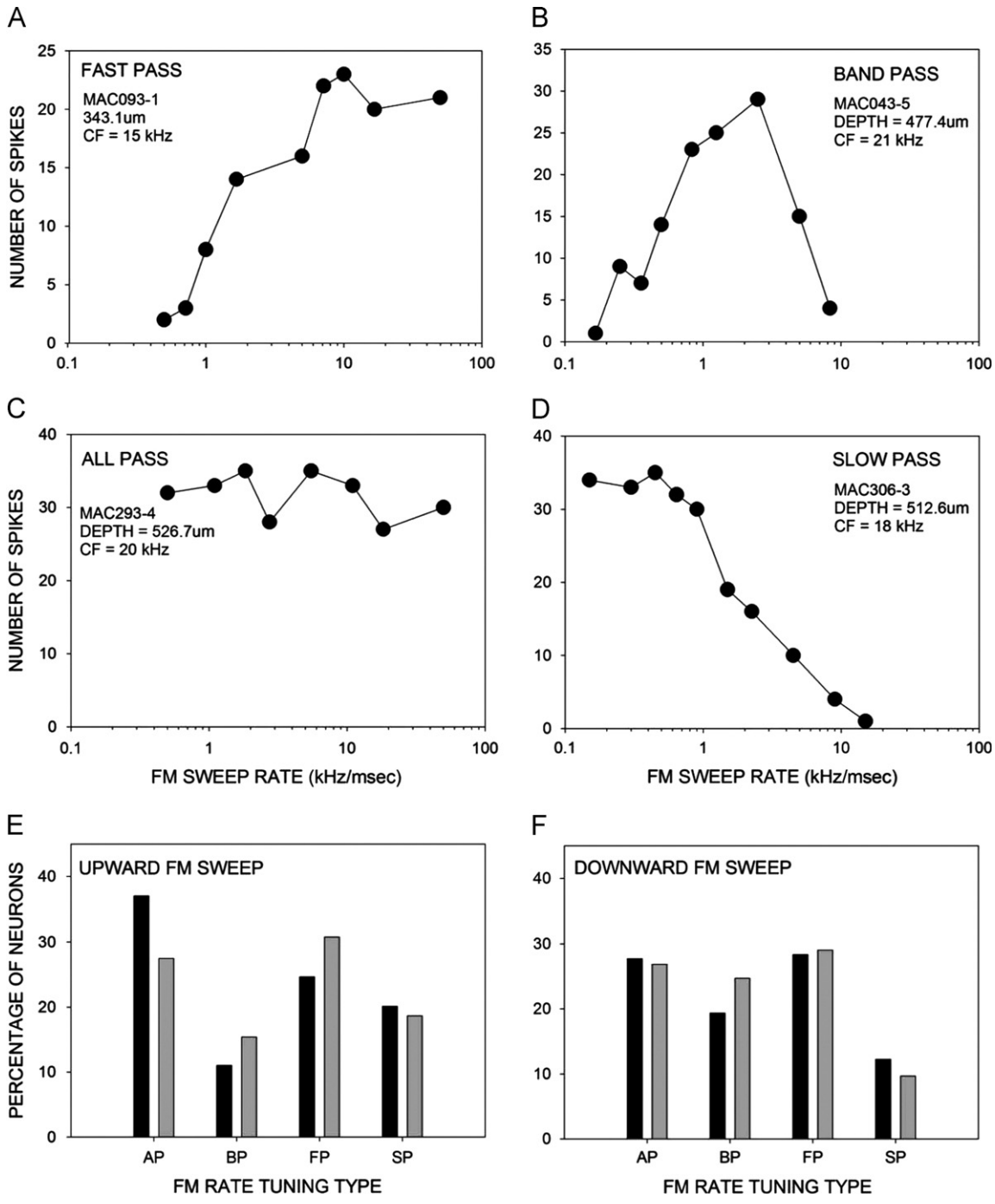

Fig. 4 – Neuron classification according to FM sweep rate selectivity (A–D) and the distribution of FM rate selectivity classes in WT and KO cortex (E, F). Neurons that favored fast rates were classified as 'fast pass' (A); neurons that responded best to an intermediate range of sweep rates were classified as 'band pass' (B); neurons that did not respond preferentially to any rate were 'all pass' (C); and, neurons that preferred slow rates were 'slow pass' (D). In A–D, 'Number of spikes' is in response to 20 repetitions of each sweep. FM sweep rate selectivity was measured in response to upward and downward FM sweeps. There was no difference in the distribution of FM rate selectivity classes between KO and WT mice for either upward (E) or downward (F) sweeps.

rate is present. For band-pass neurons, both 'fast' and 'slow' 50% cut-off rates are present. The 'slow' 50% rate was combined for fast-pass and band-pass neurons in the following analysis. As in the example shown (Fig. 6A), the population average 'fast' 50% cut-off rate in band-pass neurons was significantly higher in KO neurons than WT neurons (Fig. 6B, one-way ANOVA $F(3,99)=9.532$, $p<0.001$). There was no difference in the 'slow' 50% cut-off rate in band-pass and fast-pass neurons (Fig. 6C, one-way ANOVA $F(3,99)=1.768$, $p=0.158$). This asymmetric expansion of rate selectivity

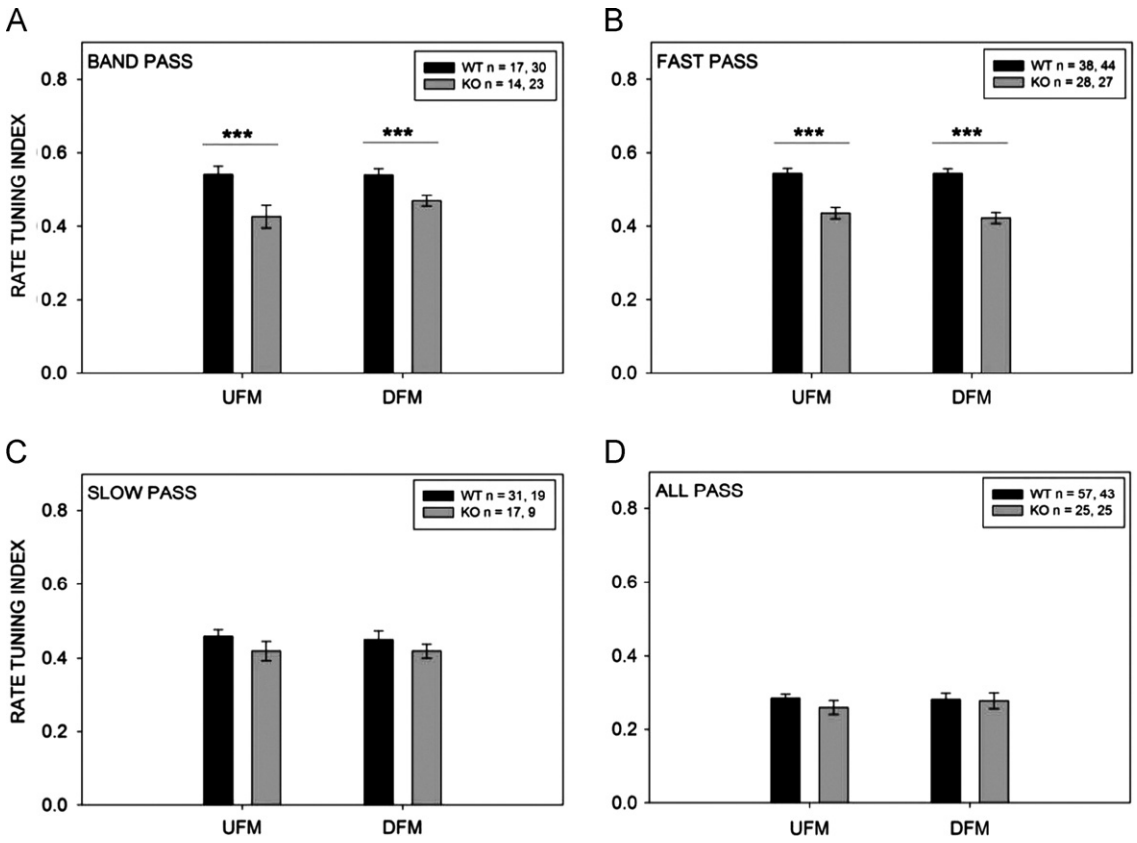

Fig. 5 – *Fmr1* KO mouse neurons show broader rate selectivity functions. Band pass (A) and fast pass (B) neurons from KO mice show decreased rate tuning index (RTI) in response to both upward and downward FM sweeps. Slow pass (C) and all pass (D) neurons, however, did not show significant difference in RTI between groups.

graphs towards the faster rates also resulted in band-pass neurons exhibiting faster best rates (Fig. 6D, one-way ANOVA $F(3,99)=2.974$, $p=0.035$). The population level differences in 50% cut-offs and best rates were similar for upward and downward sweeps.

2.4. *FM sweep direction selectivity*

Direction selectivity index (DSI) was calculated at three different ranges of rates to compare direction selectivity between WT and KO mouse neurons. DSI values closer to -1 indicate upward sweep selectivity and values closer to +1 indicate downward sweep selectivity. Up or down sweep direction selective and non-direction selective neurons were found in both WT and KO mice. Fig. 7A is an example of a WT neuron that responds preferentially to upward FM sweeps, with Fig. 7B showing a WT neuron that responds similarly to upward and downward FM sweeps. Fig. 7C shows a KO neuron that responds more strongly to downward FM sweeps, while Fig. 7D represents a KO neuron that is not selective for sweep direction. DSI was found for slow rates (0.1–1.0 kHz/ms, Fig. 8A), medium rates (1.1–3.0 kHz/ms, Fig. 8B), and fast rates (3.1–10.0 kHz/ms, Fig. 8C). There were no significant differences between the WT and KO groups within each sweep rate range (Fig. 8D, one-way ANOVA). Comparing DSI according to FM sweep rate selectivity type (FP, BP, AP and SP) also did not reveal a difference in direction selectivity (data not shown). Linear regression analysis did not reveal a significant relationship between the CF and DSI value at any FM sweep rate range tested in either WT (slow $R^2=0.0143$, $p=0.220$; medium $R^2=0.0063$, $p=0.419$; fast $R^2=0.0049$, $p=0.482$) or KO (slow $R^2=0.0182$, $p=0.331$; medium $R^2=0.0075$, $p=0.509$; fast $R^2=0.0022$, $p=0.722$) mice.

3. Discussion

The goal of this study was to compare cortical responses to tones and FM sweeps between *Fmr1* KO mice and WT controls. Compared to neurons from WT mice, neurons in KO mice showed broader frequency tuning, larger response magnitude and more variability of first spike latency when tested with tones. There was no difference in minimum thresholds and in the first spike latency between the groups. In response to FM sweeps, KO neurons were less selective for sweep rates but did not show differences in direction selectivity. The reduction in rate selectivity was due to enhanced responses to fast sweep rates in KO mice. There was no difference in the slow 50% cut-off rate, a measure of neural selectivity to slower sweeps. Taken together, the data suggest changes in cortical processing of both spectral and spectro-temporal properties in the *Fmr1* KO mice. It must be noted that these data do not indicate that the auditory cortex is the origin of observed deficits as abnormal cortical responses can

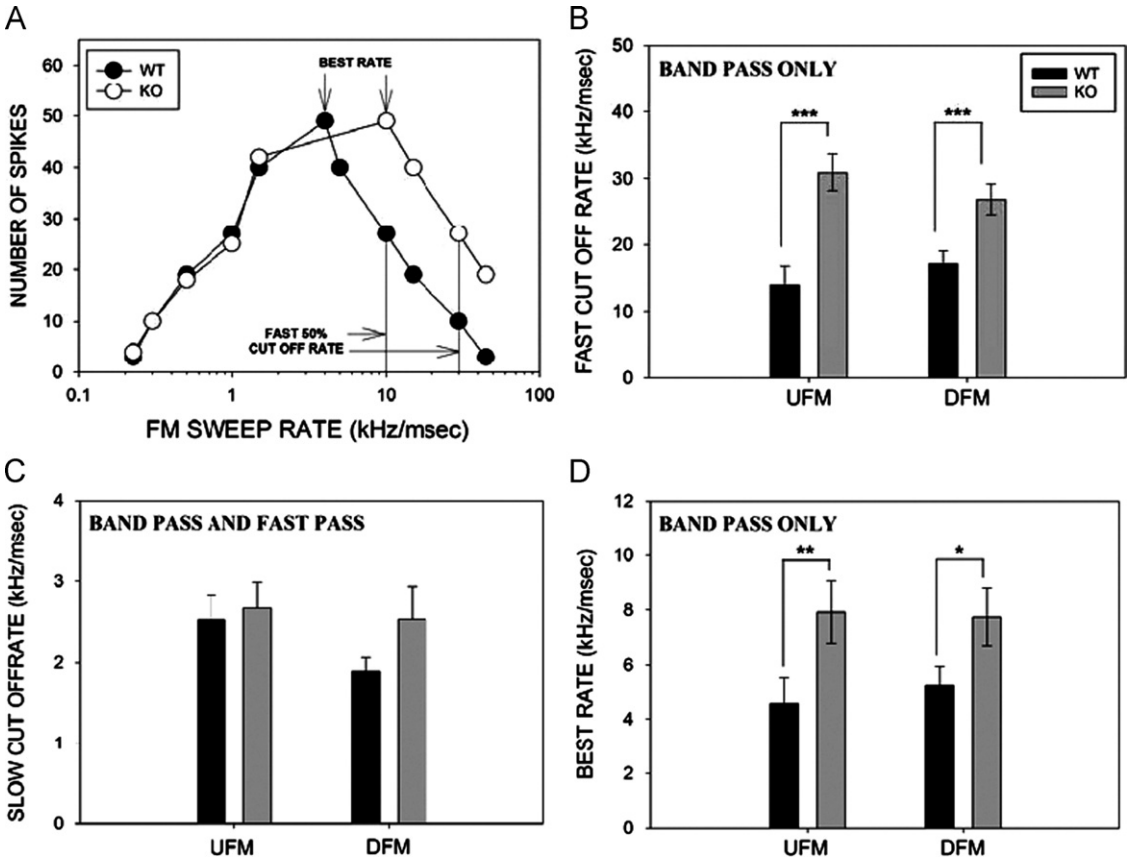

Fig. 6 – Band pass and fast pass neurons in *Fmr1* KO mice show altered rate selectivity. (A) The rate selective responses of representative BP neurons from the KO and WT mice are shown. The KO neuronal response has a higher best rate and 'fast' 50% cut off rate. The 'slow' 50% cut-off rate was not different. (B) Band pass neurons from KO mice show a greater 'fast' 50% cut off rate than WT neurons (WT: $n=31$, KO: $n=24$). (C) The 50% cut-off rate to slow sweep rates in band pass neurons and 50% cut-off rate of fast pass neurons were grouped. No significant difference was found between groups (WT: $n=70$, KO: $n=53$). (D) The best rate of band pass neurons was significantly faster in KO neurons.

be inherited from sub-cortical sites. As with other phenotypes seen in the *Fmr1* KO mice (reviewed in Bernardet and Crusio, 2006), the data do not point to gross pathology of the auditory system.

3.1. *Enhanced responses to pure tones and broader frequency tuning*

Neurons in the KO mice respond more than WT neurons to CF tone stimulation at similar sound levels. Over-active neurons may be associated with auditory behavior changes seen in *Fmr1* KO mice (Chen and Toth, 2001) and enhanced auditory ERP responses in humans with FXS (Castren et al., 2003; Van der Molen et al., 2012a, 2012b). *Fmr1* KO mice are susceptible to audiogenic seizures and show aberrant prepulse inhibition and auditory startle responses (Chen and Toth, 2001; Nielsen et al., 2002). When FMRP is reintroduced to *Fmr1* KO mice, the number of audiogenic seizures is reduced (Musumeci et al., 2007). Whether neural responses to sounds are also reduced under such conditions will be important to test in the future. The larger response magnitude, particularly during the latter portion of the response window, may arise due to increased intrinsic excitability and/or reduced synaptic inhibition in response to a CF tone (de Vrij et al., 2008; Errijgers et al., 2008; Levenga et al., 2011; Olmos-Serrano et al., 2011; Thomas et al., 2012). Gibson et al. (2008) found that neurons of the *Fmr1* KO somatosensory cortex were intrinsically more excitable then cells found in control mice. Gross et al., (2011) suggested that increased excitability may be related to impaired regulation of potassium ion channels in the KO mice. In *Fmr1* KO mice, excitatory neurons produced more frequent and prolonged UP states (Gibson et al., 2008). Of particular note, loss of *Fmr1* alone, rather than impaired inhibition, was shown to produce prolonged UP states (Hays et al., 2011).

Wehr and Zador (2001) showed that the onset response to a tone is an excitatory post-synaptic potential followed by a delayed inhibitory post-synaptic potential. The function of the latter was to reduce responses following the initial burst. Increased response magnitude may therefore result from a reduction in this CF-generated inhibition. Deficits are present in cortical $GABA_A$ receptor structure and function in *Fmr1* KO mice. Altered $GABA_A$ receptor subunit expression and unusual inhibitory interneuron activity has been found in *Fmr1* KO mice (D'Hulst et al., 2006, 2009). Functionally abnormal inhibition has also been found in *Fmr1* KO mice. Whole cell

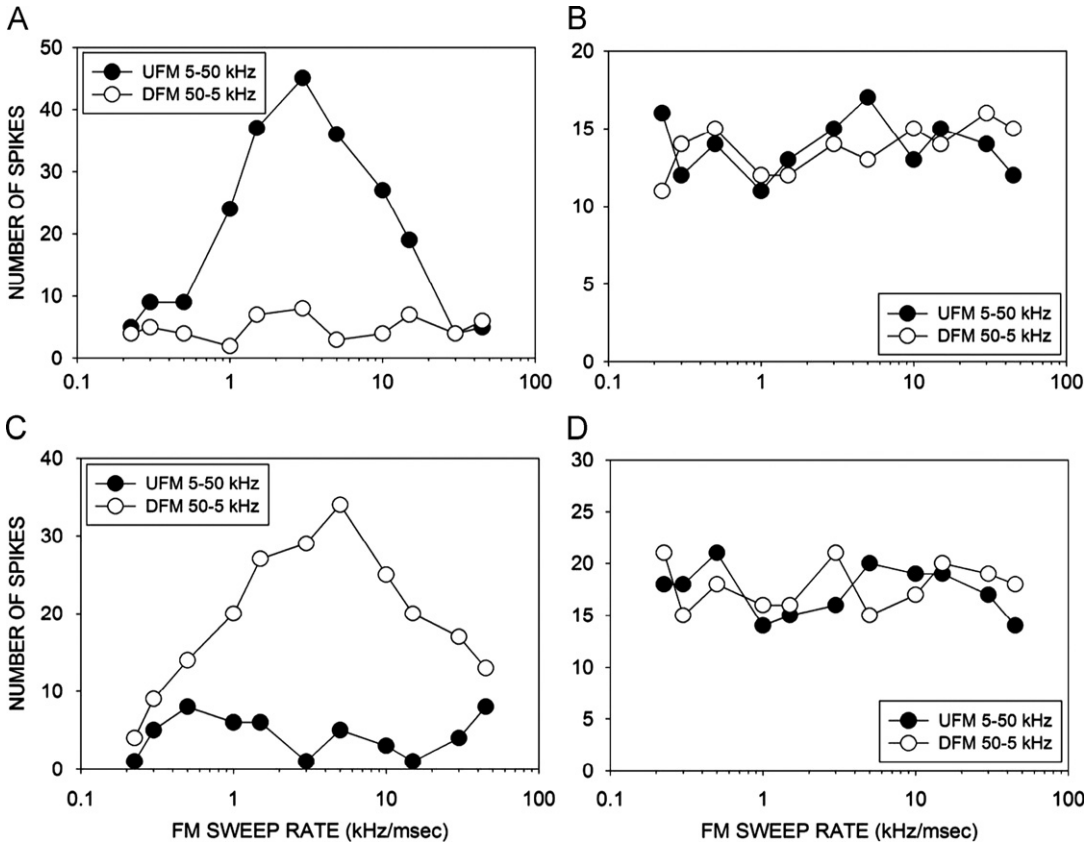

Fig. 7 – Direction selective and non-direction selective neurons in control and *Fmr1* KO mice. DSI was calculated by finding the area under the curve at three different ranges of FM sweep rates (slow, medium, and fast) in response to both upward and downward FM sweeps. Both CT (A, B) and KO (C, D) neurons displayed direction selective (A and C) and non-direction selective responses (B, D).

recordings in response to stimulation of thalamocortical axons projecting to the somatosentory cortex of *Fmr1* KO mice show decreased excitatory drive to fast spiking inhibitory interneurons, resulting in decreased inhibitory output (Gibson et al., 2008). Impaired inhibitory interneuron network function was also found in *Fmr1* KO mice (Paluszkiewicz et al., 2011). Whole cell recordings performed on pyramidal cells in the somatosensory cortex of *Fmr1* KO mice showed decreased activation of somatostatin expressing low-threshold-spiking interneurons upon mGluR1/5 stimulation, which resulted in less synchronized synaptic inhibition, and less coordinated pyramidal cell spiking (Paluszkiewicz et al., 2011). Such changes in the auditory cortex may explain the observed variability in first-spike latency in the KO mice. It is also conceivable that excessive dendritic spine formation, a consistent phenotype in *Fmr1* KO mice and in FXS patients, could produce altered cortical circuitry in *Fmr1* KO mice (Comery et al., 1997; Irwin et al., 2002; Galvez et al., 2003; McKinney et al., 2005; Till et al., 2012).

The broadened frequency tuning in the KO mice may also be explained by a reduction in inhibition or increased intrinsic excitability. Frequency tuning is shaped by overlapping inhibitory and excitatory inputs (Wehr and Zador, 2003; Wu et al., 2008; Tan and Wehr, 2009). Iontophoresis of GABA receptor antagonists on neurons cause expansion of tuning curves in many cases indicating contribution of inhibitory input in shaping frequency tuning (Muller and Scheich, 1988; Fuzessery and Hall, 1996; Wang et al., 2002; Kaur et al., 2004; Wu et al., 2008). Increased intrinsic excitability may also cause broader frequency tuning through stronger responses elicited by frequencies near the edges of the tuning curve.

3.2. *FM sweep rate and direction selectivity*

Using FM sweeps as stimuli, we did not find any difference in the distribution of FM rate tuning type, but we did find altered rate tuning in *Fmr1* KO mice. Band pass and fast pass neurons in *Fmr1* KO mice were less sharply rate tuned, and were tuned to faster rates than wild type mouse neurons. All pass and slow pass neurons were unaffected in *Fmr1* KO mice. In BP and FP neurons, the shift to faster best rates and fast 50% cutoff rates may be attributed to broader frequency tuning. In a study of the AI response properties of squirrel monkeys, a significant correlation was found between the bandwidth of frequency tuning and best sweep rate. Neurons that were more broadly tuned tended to respond maximally to faster FM sweep rates (Godey et al., 2005). Though no correlation between tuning bandwidth and rate tuning index (RTI) was found in the squirrel monkey (Godey et al., 2005), research done in the auditory cortex of chinchillas showed a negative correlation between frequency tuning and RTI (Brown and

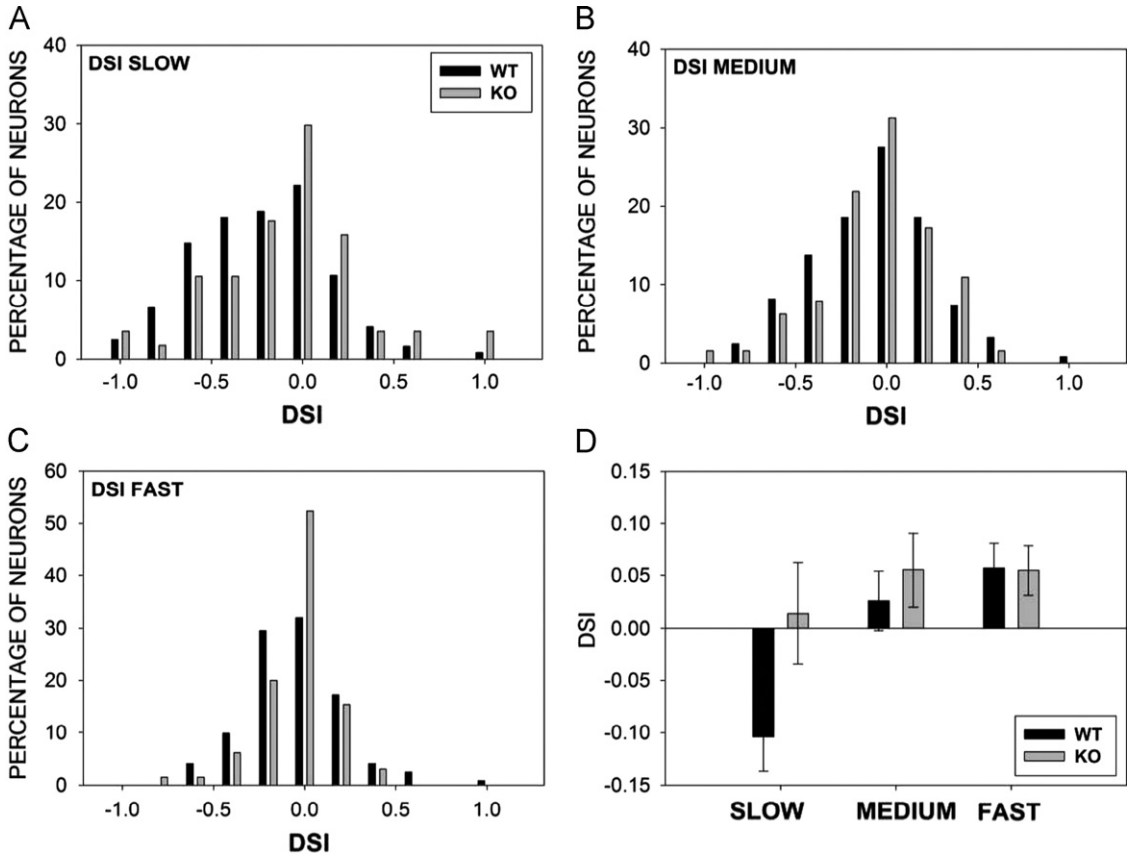

Fig. 8 – No differences in FM direction selectivity between *Fmr1* KO and wild type mice. Direction selectivity index (DSI) was used to assess direction selectivity in neurons of WT and KO mice. DSI was calculated at slow (A), medium (B), and fast (C) ranges of FM sweep rates. (D) DSI in WT and KO mouse neurons was not significantly different at any rate range tested (WT: $n=131$, KO: $n=68$).

Harrison, 2009) implying that neurons with narrower frequency tuning are likely to be more selective for sweep rates than more broadly tuned neurons (Brown and Harrison, 2009). Consistent with these findings, *Fmr1* KO mouse neurons demonstrate broader frequency tuning, faster best FM sweep rates, and reduced rate tuning overall.

There was no difference in FM sweep direction selectivity between the two groups. A comparison of Fig. 8A, B and C shows that more direction selective responses (DSI > 0.3 or DSI < −0.3) are present when tested with slow sweep rates. The histogram compresses towards DSI = 0 at faster sweep rates. Asymmetries in spectrotemporal interactions between inhibition and excitation and the relative amplitudes of the underlying post-synaptic conductance are known to shape FM sweep rate and direction selectivity (Zhang et al., 2003; Razak and Fuzessery, 2006; Sadagopan and Wang, 2010; Gittelman and Pollak, 2011). The changes in inhibitory circuitry outlined above may at least partly underlie observed differences in sweep rate selectivity. This is currently being tested. Direction selectivity, on average, is poor in mouse cortex and does not change in the KO mice.

3.3. *Methodological considerations*

The combination of urethane and xylazine used to anesthetize mice will alter auditory responses. Urethane acts by enhancing $GABA_A$, glycine, and acetylcholine receptor function and reducing NMDA and AMPA receptor function (Hara and Harris, 2002). Xylazine works by inhibiting noradrenergic transmission (Hsu, 1981). Urethane and xylazine may reduce neuronal response magnitude, but as the anesthetic regimen was applied to both wild type and *Fmr1* KO mice, the differences in selectivity observed here are unlikely to be an artifact of anesthesia. A second caveat to consider while interpreting data is the fact that littermate controls were not used in this study. Differences in maternal pup care may result from *Fmr1* KO mice being raised by *Fmr1* KO mothers and wild type mice being raised by wild type mothers. Though research is limited, differences in maternal care of pups have not been reported in *Fmr1* KO mice to our knowledge. We did not observe differences in body weight between the groups. The KO and WT pups were raised in the same vivarium room (and shelves) and were therefore in similar auditory environments until the day of electrophysiology.

3.4. *Conclusions*

Impaired spectral resolution, greater response magnitude, decreased temporal fidelity of responses and altered FM sweep rate selectivity may underlie auditory processing deficits seen in FXS patients. Individuals with FXS show excessive ERP responses to pure tones (Rojas et al., 2001;

Castren et al., 2003; Van der Molen et al., 2012a, 2012b). Notably, FXS patients consistently show enhancement of components that are associated with early processing of auditory stimuli (Rojas et al., 2001; Castren et al., 2003; Van der Molen et al., 2012a, 2012b). Subsequent aberrations in auditory processing may stem from improper sound-memory trace formation, and may underlie some aspects of FXS-related language abnormalities (Cone-Wesson and Wunderlich, 2003; Naatanen et al., 2007, 2011). Our data suggest that a battery of auditory tests that encompass a broad range of spectral, temporal and spectrotemporal complexities may provide a potentially rich source of relevant biomarkers in FXS. Our data also show that the *Fmr1* KO mouse is a useful model to study auditory processing-based biomarkers relevant to FXS. Future studies will investigate the development of auditory processing in the KO mice, the role of experience-dependent plasticity and the effects of potential therapeutics on auditory responses.

4. Experimental procedure

4.1. Mice

Fmr1 KO mice are available on both FVB and C57bl/6 background strains (Bernardet and Crusio, 2006). The latter strain is subject to accelerated hearing loss and observed results in this study may be confounded by peripheral changes (Spongr et al., 1997). FVB mice do not show early onset hearing loss and hearing thresholds are low up to at least 7 months of age (Zheng et al., 1999). Therefore, we chose the FVB strain in this study. All mice used here were between 1 and 4 months old. FVB.129P2-*Fmr1*^{tm4Cgr} (*Fmr1* KO) and FVB.129P2-*Pde6b*$^{+}$*Tyr*$^{c-ch}$/AntJ control mice were obtained from Jackson Laboratories and housed in an accredited vivarium with 12 h light/dark cycle. All studies were performed in accordance with the National Institutes of Health and with Institutional Animal Care and Use Committee guidelines. Mice were housed with 1–3 littermates and fed *ad libitum*. Fifty control mice and 37 *Fmr1* KO mice (both males and females) were used in this study.

4.2. Surgery

Mice were anesthetized with a combination of 1 g/kg urethane and 20 mg/kg xylazine. A toe pinch was administered every half hour to assess the anesthetic state, and supplemental doses of urethane and xylazine were given as needed. When an areflexic anesthetic state was reached, a midline incision was made to expose the skull. The skull was then cleaned and the temporalis muscle was reflected. A dental drill was used to perform a craniotomy to expose the auditory cortex, identified using vascular landmarks and the Paxinos mouse brain atlas. At the conclusion of the experiment, mice were euthanized with a lethal dose of 125 mg/kg sodium pentobarbital.

4.3. Electrophysiology

Mice were secured on a bite bar and placed in a stereotaxic apparatus (model 930; Kopf, Tujunga, CA). Experiments were performed in a sound-attenuated chamber lined with anechoic foam (Gretch-Ken Industries, Lakeview, OR). Electrophysiological recordings were obtained using glass electrodes filled with 1 M NaCl (impedance 2–10 MΩ). Electrodes were maintained orthogonal to the auditory cortex and driven into the cortex using a Kopf direct drive 2660 micropositioner. Recordings were gathered at depths of 200–700 μm (Table 1) with most neurons recorded between 300–700 μm. The majority of our recordings were therefore gathered in the granular (layers III and IV) and infragranular (layers V and VI) layers of the auditory cortex (Anderson et al., 2009; Christianson et al., 2011). Single unit recordings were isolated using a window discriminator and identified by the waveform displayed and consistency of the spike amplitude. Each stimulus was repeated 20 times and the number of action potentials elicited within 200 ms of stimulus onset was counted. There was very little to no spontaneous activity in the anesthetized cortex.

4.4. Acoustic stimulation

Sounds were presented through a free-field speaker (LCY-K100 ribbon tweeter; Madisound, Middleton, WI) maintained 6 in. and 45° from the left ear. All recordings were obtained from the right cortex. A1/AAF location was confirmed using tonotopy (Trujillo et al., 2011), vascular landmarks and robust, short latency responses to pure tones. The frequency response of the sound delivery system, assessed with a one-fourth inch Bruel and Kjaer microphone and measuring amplifier, was flat within ±3 dB between 7 and 40 kHz. The roll-off at higher frequencies was gradual at ~20 dB/octave. Acoustic stimulation and data acquisition were done with custom-written software (Batlab, Dr. Dan Gans, Kent State University, OH) and a Microstar digital signal processing board. Sound intensity was controlled by programmable attenuators (PA5; Tucker-Davis Technologies, Gainesville, FL).

4.5. Frequency tuning

Isolated single units were probed with 50 ms pure tones (1 ms rise/fall times). At a given intensity, the frequency of the tone was increased in 1 or 5 kHz increments. A neuron was counted as responding to a given frequency if it produced action potentials to at least four of five consecutive stimulus presentations. Frequencies between 5 and 50 kHz were tested because the vast majority of neurons in the lemniscal auditory pathway of mice are tuned <50 kHz (Portfors and Felix, 2005; Willott, 2006). Both A1 and AAF are considered core auditory cortical fields in the lemniscal pathway. Tone intensity was increased or decreased by 10 dB to determine frequency-intensity tuning curves. The range of intensity tested was between 30 and 90 dB SPL. The characteristic frequency (CF) was defined as the frequency to which the neuron responded at the lowest intensity tested. The intensity level at which CF was revealed was termed 'minimum threshold'. Q-values were used to compare the tuning curve bandwidths by dividing the CF by the bandwidth of tuning at 10, 20, or 30 dB above the minimum threshold. Larger Q-values indicate narrower tuning curves.

4.6. Response magnitude and variability of first spike latency

In order to compare the magnitude of neuronal responses in WT and KO mouse neurons, a 10 ms single frequency tone at the CF (10–20 dB above threshold) was repeated 20 times. The total response over a 200 ms window from stimulus onset was then averaged over the 20 trials. To assess variability in the first spike latency in response to repetitions of the same tone, the Fano factor was calculated for neurons from both WT and KO mice using the following equation:

$$\text{Fano Factor} = \text{variance}/\text{mean}$$

In this equation, 'variance' refers to the variance of first spike latency over 20 repetitions of the same tone, and 'mean' is the average first spike latency.

4.7. Frequency-modulated (FM) sweep rate selectivity

FM sweeps are relatively simple sounds used to study spectrotemporal processing. Neurons sensitive to the direction and/or rate of FM sweeps are present in the mouse cortex (Trujillo et al., 2011). To test FM sweep rate selectivity, linear FM sweeps were presented at a fixed bandwidth (50→5 kHz or 5→50 kHz) and various durations. FM sweep rates (kHz/ms) were calculated by dividing the bandwidth of the sweep (kHz) by the duration of the sweep (ms). FM sweeps were presented at 10–20 dB above minimum threshold. Sweep rates between 0.2 and 45 kHz/ms were tested.

Neuronal responses to FM sweeps were classified according to four different response types: all pass (AP), band pass (BP), fast pass (FP), or slow pass (SP) (Trujillo et al., 2011). All pass neurons responded within 50% of maximum response to all FM sweep rates presented. Band pass neurons responded maximally to an intermediate range of rates, with the responses falling below 50% of the maximum at rates both greater than and less than the preferred rate. Fast pass neuron responded maximally to relatively fast rates, with response falling below 50% of the maximum as the sweep rate was decreased. Slow pass neurons responded best to relatively slow rates, with response falling below 50% as the sweep rate was increased.

The '50% cutoff rate' was calculated for FP and BP neurons. In FP neurons, the 50% cutoff rate was the rate at which the response fell to 50% of the maximum response as the sweep rate was slowed. In BP neurons there were two possible 50% cutoff rates: the 50% cutoff for increasing rates (termed 'fast 50% cut-off rate'), and the 50% cutoff for decreasing rates (termed 'slow 50% cut-off rate'). The 'best rate' of BP neurons was calculated as the geometric mean of the neuronal response at 80% of the maximum response.

A rate tuning index (RTI) was quantified to determine the degree of rate selectivity (Godey et al., 2005; Trujillo et al., 2011):

$$\text{RTI} = [n/(n-1)] \times [1-(\text{mean}/\text{maximum})]$$

where n is the number of sweep rates tested, mean is the average response across all rates presented, and maximum is the maximum response. Values closer to 1 describe neurons with a high degree of rate selectivity. A value near 0 indicates a non-selective neuron.

4.8. FM sweep direction selectivity

FM sweep direction selectivity was determined by comparing responses to linear upward and downward sweeps of the same bandwidth. The direction selectivity index (DSI) was calculated using the following equation:

$$\text{DSI} = (D-U)/(D+U)$$

D and U are the trapezoidal area under the curve in response to downward and upward FM sweeps, respectively. As direction selectivity can change with sweep rate (Zhang et al., 2003; Razak et al., 2008), DSI was evaluated at three different ranges of rate. DSI was found for 'slow' rates (0.18–1 kHz/ms), for 'medium' rates (1.1–3.0 kHz/ms), and for 'fast' rates (3.1–10.0 kHz/ms). DSI values near 1 suggest a preference for downward FM sweeps, while DSI values near −1 suggest a preference for upward FM sweeps.

Acknowledgments

This work was supported by the FRAXA Research Foundation. We thank members of the Razak lab for useful discussions on the data and the manuscript. We also thank Dr. Iryna Ethell for providing mice for experiments and discussions of the data.

REFERENCES

Anderson, L.A., Christianson, G.B., Linden, J.F., 2009. Mouse auditory cortex differs from visual and somatosensory cortices in the laminar distribution of cytochrome oxidase and acetylcholinesterase. Brain Res. 1252, 130–142.

Barnes, E., Roberts, J., Long, S.H., Martin, G.E., Berni, M.C., Mandulak, K.C., Sideris, J., 2009. Phonological accuracy and intelligibility in connected speech of boys with fragile X syndrome or Down syndrome. J. Speech Lang. Hear. Res. 52, 1048–1061.

Bassell, G.J., Warren, S.T., 2008. Fragile X syndrome: loss of local mRNA regulation alters synaptic development and function. Neuron 60, 201–214.

Bernardet, M., Crusio, W.E., 2006. Fmr1 KO mice as a possible model of autistic features. Sci. World J. 6, 1164–1176.

Brown, T.A., Harrison, R.V., 2009. Responses of neurons in chinchilla auditory cortex to frequency-modulated tones. J. Neurophysiol. 13, 2017–2029.

Castren, M., Paakkonen, A., Tarkka, I.M., Ryynanen, M., Partanen, J., 2003. Augmentation of auditory N1 in children with fragile X syndrome. Brain Topogr. 15, 165–171.

Chen, L., Toth, M., 2001. Fragile X mice develop sensory hyperreactivity to auditory stimuli. Neuroscience 103, 1043–1050.

Christianson, G.B., Sahani, M., Linden, J.F., 2011. Depth-dependent temporal response properties in core auditory cortex. J. Neurosci. 31, 12837–12848.

Comery, T.A., Harris, J.B., Willems, P.J., Oostra, B.A., Irwin, S.A., Weiler, I.J., Greenough, W.T., 1997. Abnormal dendritic spines in fragile X knockout mice: maturation and pruning deficits. Proc. Natl. Acad. Sci. U.S.A. 94, 5401–5404.

Cone-Wesson, B., Wunderlich, J., 2003. Auditory evoked potentials from the cortex: audiology applications. Curr. Opin. Otolaryngol. Head Neck Surg. 11, 372–377.

Crawley, J.N., 2007. Mouse behavioral assays relevant to the symptoms of autism. Brain Pathol. 17, 448–459.

Cruz-Martin, A., Crespo, M., Portera-Cailliau, C., 2010. Delayed stabilization of dendritic spines in fragile X mice. J. Neurosci. 30, 7793–7803.

D'Hulst, C., De Geest, N., Reeve, S.P., Van Dam, D., De Deyn, P.P., Hassan, B.A., Kooy, R.F., 2006. Decreased expression of the GABAA receptor in fragile X syndrome. Brain Res. 1121, 238–245.

D'Hulst, C., Heulens, I., Brouwer, J.R., Willemsen, R., De Geest, N., Reeve, S.P., De Deyn, P.P., Hassan, B.A., Kooy, R.F., 2009. Expression of the GABAergic system in animal models for fragile X syndrome and fragile X associated tremor/ataxia syndrome (FXTAS). Brain Res. 1253, 176–183.

de Vrij, F.M., Levenga, J., van der Linde, H.C., Koekkoek, S.K., De Zeeuw, C.I., Nelson, D.L., Oostra, B.A., Willemsen, R., 2008. Rescue of behavioral phenotype and neuronal protrusion morphology in *Fmr1* KO mice. Neurobiol. Dis. 31, 127–132.

Errijgers, V., Fransen, E., D'Hooge, R., De Deyn, P.P., Kooy, R.F., 2008. Effect of genetic background on acoustic startle response in fragile X knockout mice. Genet. Res. (Camb.) 90, 341–345.

Fidler, D.J., Philofsky, A., Hepburn, S.L., 2007. Language phenotypes and intervention planning: bridging research and practice. Ment. Retard. Dev. Disabil. Res. Rev. 13, 47–57.

Frankland, P.W., Wang, Y., Rosner, B., Shimizu, T., Balleine, B.W., Dykens, E.M., Ornitz, E.M., Silva, A.J., 2004. Sensorimotor gating abnormalities in young males with fragile X syndrome and *Fmr1*-knockout mice. Mol. Psychiatry 9, 417–425.

Fuzessery, Z.M., Hall, J.C., 1996. Role of GABA in shaping frequency tuning and creating FM sweep selectivity in the inferior colliculus. J. Neurophysiol. 76, 1059–1073.

Galvez, R., Gopal, A.R., Greenough, W.T., 2003. Somatosensory cortical barrel dendritic abnormalities in a mouse model of the fragile X mental retardation syndrome. Brain Res. 971, 83–89.

Gibson, J.R., Bartley, A.F., Hays, S.A., Huber, K.M., 2008. Imbalance of neocortical excitation and inhibition and altered UP states reflect network hyperexcitability in the mouse model of fragile X syndrome. J. Neurophysiol. 100, 2615–2626.

Gittelman, J.X., Pollak, G.D., 2011. It's about time: how input timing is used and not used to create emergent properties in the auditory system. J. Neurosci. 31, 2576–2583.

Godey, B., Atencio, C.A., Bonham, B.H., Schreiner, C.E., Cheung, S.W., 2005. Functional organization of squirrel monkey primary auditory cortex: responses to frequency-modulation sweeps. J. Neurophysiol. 94, 1299–1311.

Grossman, A.W., Elisseou, N.M., McKinney, B.C., Greenough, W.T., 2006. Hippocampal pyramidal cells in adult *Fmr1* knockout mice exhibit an immature-appearing profile of dendritic spines. Brain Res. 1084, 158–164.

Grossman, A.W., Aldridge, G.M., Lee, K.J., Zeman, M.K., Jun, C.S., Azam, H.S., Arii, T., Imoto, K., Greenough, W.T., Rhyu, I.J., 2010. Developmental characteristics of dendritic spines in the dentate gyrus of *Fmr1* knockout mice. Brain Res. 1355, 221–227.

Hagerman, P.J., 2008. The fragile X prevalence paradox. J. Med. Genet. 45, 498–499.

Hagerman, R.J., Amiri, K., Cronister, A., 1991. Fragile X checklist. Am. J. Med. Genet. 38, 283–287.

Hagerman, R.J., Jackson 3rd, A.W., Levitas, A., Rimland, B., Braden, M., 1986. An analysis of autism in fifty males with the fragile X syndrome. Am. J. Med. Genet. 23, 359–374.

Hall, S.S., Walter, E., Sherman, E., Hoeft, F., Reiss, A.L., 2011. The neural basis of auditory temporal discrimination in girls with fragile X syndrome. J. Neurodev. Disord. 1, 91–99.

Hanson, D.M., Jackson 3rd, A.W., Hagerman, R.J., 1986. Speech disturbances (cluttering) in mildly impaired males with the Martin–Bell/fragile X syndrome. Am. J. Med. Genet. 23, 195–206.

Hara, K., Harris, R.A., 2002. The anesthetic mechanism of urethane: the effects on neurotransmitter-gated ion. Anesth. Analg. 94, 313–318.

Hays, S.A., Huber, K.M., Gibson, J.R., 2011. Altered neocortical rhythmic activity states in *Fmr1* KO mice are due to enhanced mGluR5 signaling and involve changes in excitatory circuitry. J. Neurosci. 31, 14223–14234.

Hazlett, H.C., Poe, M.D., Lightbody, A.A., Styner, M., Macfall, J.R., Reiss, A.L., Piven, J., 2012. Trajectories of early brain volume development in fragile X syndrome and autism. J. Am. Acad. Child Adolescent Psychiatry 51, 921–933.

Hessl, D., Berry-Kravis, E., Cordeiro, L., Yuhas, J., Ornitz, E.M., Campbell, A., Chruscinski, E., Hervey, C., Long, J.M., Hagerman, R.J., 2009. Prepulse inhibition in fragile X syndrome: feasibility, reliability, and implications for treatment. Am. J. Med. Genet. B Neuropsychiatry Genet. 150B, 545–553.

Hsu, W.H., 1981. Xylazine-induced depression and its antagonism by alpha adrenergic blocking. J. Pharmacol. Exp. Ther. 218, 188–192.

Irwin, S.A., Idupulapati, M., Gilbert, M.E., Harris, J.B., Chakravarti, A.B., Rogers, E.J., Crisostomo, R.A., Larsen, B.P., Mehta, A., Alcantara, C.J., Patel, B., Swain, R.A., Weiler, I.J., Oostra, B.A., Greenough, W.T., 2002. Dendritic spine and dendritic field characteristics of layer V pyramidal neurons in the visual cortex of fragile-X knockout mice. Am. J. Med. Genet. 111, 140–146.

Kaur, S., Lazar, R., Metherate, R., 2004. Intracortical pathways determine breadth of subthreshold frequency receptive fields in primary auditory cortex. J. Neurophysiol. 91, 2551–2567.

Largo, R.H., Schinzel, A., 1985. Developmental and behavioural disturbances in 13 boys with fragile X syndrome. Eur. J. Pediatr. 143, 269–275.

Levenga, J., Hayashi, S., de Vrij, F.M., Koekkoek, S.K., van der Linde, H.C., Nieuwenhuizen, I., Song, C., Buijsen, R.A., Pop, A.S., Gomezmancilla, B., Nelson, D.L., Willemsen, R., Gasparini, F., Oostra, B.A., 2011. AFQ056, a new mGluR5 antagonist for treatment of fragile X syndrome. Neurobiol. Dis. 42, 311–317.

McKinney, B.C., Grossman, A.W., Elisseou, N.M., Greenough, W.T., 2005. Dendritic spine abnormalities in the occipital cortex of C57BL/6 *Fmr1* knockout mice. Am. J. Med. Genet. B. Neuropsychiatry Genet. 136B, 98–102.

Miller, L.J., McIntosh, D.N., McGrath, J., Shyu, V., Lampe, M., Taylor, A.K., Tassone, F., Neitzel, K., Stackhouse, T., Hagerman, R.J., 1999. Electrodermal responses to sensory stimuli in individuals with fragile X syndrome: a preliminary report. Am. J. Med. Genet. 83, 268–279.

Mineur, Y.S., Sluyter, F., de Wit, S., Oostra, B.A., Crusio, W.E., 2002. Behavioral and neuroanatomical characterization of the *Fmr1* knockout mouse. Hippocampus 12, 39–46.

Muller, C.M., Scheich, H., 1988. Contributions of GABAergic inhibition to the response characteristics of auditory units in the avian forebrain. J. Neurophysiol. 59, 1673–1689.

Musumeci, S.A., Bosco, P., Calabrese, G., Bakker, C., De Sarro, G.B., Elia, M., Ferri, R., Oostra, B.A., 2000. Audiogenic seizures susceptibility in transgenic mice with fragile X syndrome. Epilepsia 41, 19–23.

Musumeci, S.A., Calabrese, G., Bonaccorso, C.M., D'Antoni, S., Brouwer, J.R., Bakker, C.E., Elia, M., Ferri, R., Nelson, D.L., Oostra, B.A., Catania, M.V., 2007. Audiogenic seizure susceptibility is reduced in fragile X knockout mice after introduction of *FMR1* transgenes. Exp. Neurol. 203, 233–240.

Naatanen, R., Kujala, T., Winkler, I., 2011. Auditory processing that leads to conscious perception: a unique window to central auditory processing opened by the mismatch negativity and related responses. Psychophysiology 48, 4–22.

Naatanen, R., Paavilainen, P., Rinne, T., Alho, K., 2007. The mismatch negativity (MMN) in basic research of central auditory processing: a review. Clin. Neurophysiol. 118, 2544–2590.

Nielsen, D.M., Derber, W.J., McClellan, D.A., Crnic, L.S., 2002. Alterations in the auditory startle response in *Fmr1* targeted mutant mouse models of fragile X syndrome. Brain Res. 927, 8–17.

O'Connor, K., 2012. Auditory processing in autism spectrum disorder: a review. Neurosci. Biobehav. Rev. 36, 836–854.

O'Donnell, W.T., Warren, S.T., 2002. A decade of molecular studies of fragile X syndrome. Annu. Rev. Neurosci. 25, 315–338.

Olmos-Serrano, J.L., Corbin, J.G., Burns, M.P., 2011. The GABA(A) receptor agonist THIP ameliorates specific behavioral deficits in the mouse model of fragile X syndrome. Dev. Neurosci. 33, 395–403.

Paluszkiewicz, S.M., Olmos-Serrano, J.L., Corbin, J.G., Huntsman, M.M., 2011. Impaired inhibitory control of cortical synchronization in fragile X syndrome. J. Neurophysiol. 106, 2264–2272.

Pan,F., Aldridge,G.M., Greenough,W.T., Gan,W.B., 2010. Dendritic spine instability and insensitivity to modulation by sensory experience in a mouse model of fragile X syndrome. In: Proceedings of the National Academy of Sciences of the United States of America 107, 17768–17773.

Portfors, C.V., Felix, R.A., 2005. Spectral integration in the inferior colliculus of the CBA/CaJ mouse. Neuroscience 136, 1159–1170.

Razak, K.A., Fuzessery, Z.M., 2006. Neural mechanisms underlying selectivity for the rate and direction of frequency-modulated sweeps in the auditory cortex of the pallid bat. J. Neurophysiol. 96, 1303–1319.

Razak, K.A., Richardson, M.D., Fuzessery, Z.M., 2008. Experience is required for the maintenance and refinement of FM sweep selectivity in the developing auditory cortex. Proc. Natl. Acad. Sci. U.S.A. 105, 4465–4470.

Reiss, A.L., Lee, J., Freund, L., 1994. Neuroanatomy of fragile X syndrome: the temporal lobe. Neurology 44, 1317–1324.

Roberts, J.E., Mirrett, P., Burchinal, M., 2001. Receptive and expressive communication development of young males with fragile X syndrome. Am. J. Ment. Retard. 106, 216–230.

Roberts, J.E., Hennon, E.A., Price, J.R., Dear, E., Anderson, K., Vandergrift, N.A., 2007. Expressive language during conversational speech in boys with fragile X syndrome. Am. J. Ment. Retard. 112, 1–17.

Rojas, D.C., Benkers, T.L., Rogers, S.J., Teale, P.D., Reite, M.L., Hagerman, R.J., 2001. Auditory evoked magnetic fields in adults with fragile X syndrome. Neuroreport 12, 2573–2576.

Rotschafer, S.E., Trujillo, M.S., Dansie, L.E., Ethell, I.M., Razak, K.A., 2012. Minocycline treatment reverses ultrasonic vocalization production deficit in a mouse model of fragile X Syndrome. Brain Res. 1439, 7–14.

Rubenstein, J.L., Merzenich, M.M., 2003. Model of autism: increased ratio of excitation/inhibition in key neural systems. Genes Brain Behav. 2, 255–267.

Sadagopan, S., Wang, X., 2010. Contribution of inhibition to stimulus selectivity in primary auditory cortex of awake primates. J. Neurosci. 30, 7314–7325.

Scherg, M., von Cramon, D., 1986. Psychoacoustic and electrophysiologic correlates of central hearing disorders in man. Eur. Arch. Psychiatry Neurol. Sci. 236, 56–60.

Spencer, C.M., Alekseyenko, O., Serysheva, E., Yuva-Paylor, L.A., Paylor, R., 2005. Altered anxiety-related and social behaviors in the *Fmr1* knockout mouse model of fragile X syndrome. Genes Brain Behav. 4, 420–430.

Spongr, V.P., Flood, D.G., Frisina, R.D., Salvi, R.J., 1997. Quantitative measures of hair cell loss in CBA and C57BL/6 mice throughout their life spans. J. Acoust. Soc. Am. 101, 3546–3553.

Strumbos, J.G., Brown, M.R., Kronengold, J., Polley, D.B., Kaczmarek, L.K., 2010. Fragile X mental retardation protein is required for rapid experience-dependent regulation of the potassium channel Kv3.1b. J. Neurosci. 30, 10263–10271.

Tan, A.Y., Wehr, M., 2009. Balanced tone-evoked synaptic excitation and inhibition in mouse auditory cortex. Neuroscience 163, 1302–1315.

Thomas, A.M., Bui, N., Perkins, J.R., Yuva-Paylor, L.A., Paylor, R., 2012. Group I metabotropic glutamate receptor antagonists alter select behaviors in a mouse model for fragile X syndrome. Psychopharmacology (Berlin) 219, 47–58.

Till, S.M., Wijetunge, L.S., Seidel, V.G., Harlow, E., Wright, A.K., Bagni, C., Contractor, A., Gillingwater, T.H., Kind, P.C., 2012. Altered maturation of the primary somatosensory cortex in a mouse model of fragile X syndrome. Hum. Mol. Genet. 21, 2143–2156.

Trujillo, M., Measor, K., Carrasco, M.M., Razak, K.A., 2011. Selectivity for the rate of frequency-modulated sweeps in the mouse auditory cortex. J. Neurophysiol. 106, 2825–2837.

Van der Molen, M.J., Van der Molen, M.W., Ridderinkhof, K.R., Hamel, B.C., Curfs, L.M., Ramakers, G.J., 2012a. Auditory change detection in fragile X syndrome males: a brain potential study. Clin. Neurophysiol. 123, 1309–1318.

Van der Molen, M.J., Van der Molen, M.W., Ridderinkhof, K.R., Hamel, B.C., Curfs, L.M., Ramakers, G.J., 2012b. Auditory and visual cortical activity during selective attention in fragile X syndrome: a cascade of processing deficiencies. Clin. Neurophysiol. 123, 720–729.

Wang, J.A., McFadden, S.L., Caspary, D., Salvi, R., 2002. Gamma-aminobutyric acid circuits shape response properties of auditory cortex neurons. Brain Res. 944, 219–231.

Wehr, M., Zador, A.M., 2003. Balanced inhibition underlies tuning and sharpens spike timing in auditory cortex. Nature 426, 442–446.

Willott, J.F., 2006. Measurement of the auditory brainstem response (ABR) to study auditory sensitivity in mice. Curr. Protocols Neurosci. Chapter 8: Unit 8 21B.

Wisniewski, K.E., Segan, S.M., Miezejeski, C.M., Sersen, E.A., Rudelli, R.D., 1991. The Fra(X) syndrome: neurological, electrophysiological, and neuropathological abnormalities. Am. J. Med. Genet. 38, 476–480.

Wu, G.K., Arbuckle, R., Liu, B.H., Tao, H.W., Zhang, L.I., 2008. Lateral sharpening of cortical frequency tuning by approximately balanced inhibition. Neuron 58, 132–143.

Yuhas, J., Cordeiro, L., Tassone, F., Ballinger, E., Schneider, A., Long, J.M., Ornitz, E.M., Hessl, D., 2011. Brief report: sensorimotor gating in idiopathic autism and autism associated with fragile X syndrome. J. Autism Dev. Disord. 41, 248–253.

Zhang, L.I., Tan, A.Y., Schreiner, C.E., Merzenich, M.M., 2003. Topography and synaptic shaping of direction selectivity in primary auditory cortex. Nature 424, 201–205.

Zheng, Q.Y., Johnson, K.R., Erway, L.C., 1999. Assessment of hearing in 80 inbred strains of mice by ABR threshold analyses. Hear. Res. 130, 94–107.